ARTICLES
https://doi.org/10.1038/s41566-020-00712-8

nature photonics

A compact and cost-effective hard X-ray free-electron laser driven by a high-brightness and low-energy electron beam

Eduard Prat[1]✉, Rafael Abela[1,6], Masamitsu Aiba[1], Arturo Alarcon[1], Jürgen Alex[1], Yunieski Arbelo[1], Christopher Arrell[1], Vladimir Arsov[1], Camila Bacellar[1,2], Carl Beard[1], Paul Beaud[1], Simona Bettoni[1], Roger Biffiger[1], Markus Bopp[1], Hans-Heinrich Braun[1], Marco Calvi[1], Ariana Cassar[3], Tine Celcer[1], Majed Chergui[2], Pavel Chevtsov[1], Claudio Cirelli[1], Alessandro Citterio[1], Paolo Craievich[1], Marta Csatari Divall[1], Andreas Dax[1], Micha Dehler[1], Yunpei Deng[1], Alexander Dietrich[1], Philipp Dijkstal[1,4], Roberto Dinapoli[1], Sladana Dordevic[1], Simon Ebner[1], Daniel Engeler[1,13], Christian Erny[1], Vincent Esposito[1,5], Eugenio Ferrari[1], Uwe Flechsig[1], Rolf Follath[1], Franziska Frei[1], Romain Ganter[1], Terence Garvey[1], Zheqiao Geng[1], Alexandre Gobbo[1], Christopher Gough[1], Andreas Hauff[1,7], Christoph P. Hauri[1,8], Nicole Hiller[1], Stephan Hunziker[1,9], Martin Huppert[1], Gerhard Ingold[1], Rasmus Ischebeck[1], Markus Janousch[1], Philip J. M. Johnson[1], Steven L. Johnson[1,4], Pavle Juranić[1], Mario Jurcevic[1], Maik Kaiser[1], Roger Kalt[1], Boris Keil[1], Daniela Kiselev[1], Christoph Kittel[1], Gregor Knopp[1], Waldemar Koprek[1], Michael Laznovsky[1], Henrik T. Lemke[1], Daniel Llorente Sancho[1], Florian Löhl[1], Alexander Malyzhenkov[1], Giulia Fulvia Mancini[1,2], Roman Mankowsky[1], Fabio Marcellini[1], Goran Marinkovic[1], Isabelle Martiel[1], Fabian Märki[1,10], Christopher J. Milne[1], Aldo Mozzanica[1], Karol Nass[1], Gian Luca Orlandi[1], Cigdem Ozkan Loch[1], Martin Paraliev[1], Bruce Patterson[1], Luc Patthey[1], Bill Pedrini[1], Marco Pedrozzi[1], Claude Pradervand[1], Peter Radi[1], Jean-Yves Raguin[1], Sophie Redford[1], Jens Rehanek[1,11], Sven Reiche[1], Leonid Rivkin[1], Albert Romann[1,14], Leonardo Sala[1], Mathias Sander[1], Thomas Schietinger[1], Thomas Schilcher[1], Volker Schlott[1], Thomas Schmidt[1], Mike Seidel[1], Markus Stadler[1,12], Lukas Stingelin[1], Cristian Svetina[1], Daniel M. Treyer[1], Alexandre Trisorio[1], Carlo Vicario[1], Didier Voulot[1], Albin Wrulich[1], Serhane Zerdane[1] and Elke Zimoch[1]

We present the first lasing results of SwissFEL, a hard X-ray free-electron laser (FEL) that recently came into operation at the Paul Scherrer Institute in Switzerland. SwissFEL is a very stable, compact and cost-effective X-ray FEL facility driven by a low-energy and ultra-low-emittance electron beam travelling through short-period undulators. It delivers stable hard X-ray FEL radiation at 1-Å wavelength with pulse energies of more than 500 μJ, pulse durations of ~30 fs (root mean square) and spectral bandwidth below the per-mil level. Using special configurations, we have produced pulses shorter than 1 fs and, in a different set-up, broadband radiation with an unprecedented bandwidth of ~2%. The extremely small emittance demonstrated at SwissFEL paves the way for even more compact and affordable hard X-ray FELs, potentially boosting the number of facilities worldwide and thereby expanding the population of the scientific community that has access to X-ray FEL radiation.

X-ray free-electron lasers (FELs) are cutting-edge research tools, used in multiple scientific fields, that allow the observation of matter on the spatial and time scales of atomic processes[1–3]. So far, these properties have facilitated new observations of structural dynamics that determine protein function[4–6], mechanisms controlling chemical bonds[7,8], and the strong interaction

[1]Paul Scherrer Institut, Villigen, Switzerland. [2]EPFL, Laboratory of Ultrafast Spectroscopy and Lausanne Centre for Ultrafast Science (LACUS), Lausanne, Switzerland. [3]University of Malta, Faculty of ICT, Msida, Malta. [4]ETH Zürich, Department of Physics, Zurich, Switzerland. [5]Stanford Institute for Materials and Energy Science, Stanford, CA, USA. [6]Present address: leadXpro AG, Villigen, Switzerland. [7]Present address: Anapico AG, Glattbrugg, Switzerland. [8]Present address: TRUMPF Schweiz AG, Baar, Switzerland. [9]Present address: Huber + Suhner AG, Herisau, Switzerland. [10]Present address: Fachhochschule Nordwestschweiz FHNW, Windisch, Switzerland. [11]Present address: Advanced Accelerator Technologies AG, PARK innovAARE, Villigen, Switzerland. [12]Present address: Matrix Elektronik AG, Ehrendingen, Switzerland. [13]Deceased: Daniel Engeler. [14]Deceased: Albert Romann. ✉e-mail: eduard.prat@psi.ch

between electronic and magnetic states, which determine processes that are interesting for energy conversion and information storage applications[9–11]. The high peak intensities and short pulse durations generated by these facilities enable room-temperature measurements of sensitive structures like G protein-coupled receptor (GPCR) membrane proteins[12–14] and have introduced an entirely new field of research on the application of nonlinear X-ray techniques[15–17].

So far, all hard X-ray FEL facilities have been based on the self-amplified spontaneous emission (SASE) process[18,19]. In 2009, the Linac Coherent Light Source (LCLS) at SLAC (USA) was the first FEL facility to produce radiation with wavelengths at the ångström level[20]. Shortly afterwards, SACLA (Japan) came into operation, producing hard X-ray FEL light with a much more compact accelerator than LCLS[21]. In the past two years, three additional hard X-ray sources began operation: PAL-XFEL (South Korea)[22], featuring excellent timing jitter at the femtosecond level, the European XFEL (Germany)[23], tremendously increasing the number of pulses per second thanks to its superconducting radiofrequency (RF) technology, and SwissFEL, a compact, stable and cost-effective facility driven by a high-brightness and low-energy electron beam. In this Article, we present the first lasing results of SwissFEL at the Paul Scherrer Institute in Villigen (Switzerland). The construction of SwissFEL began in 2013, first lasing at a relatively low energy was achieved in 2016, most of the beam commissioning took place in 2017, and a pilot phase of first scientific experiments lasted from the end of 2017 through 2018, before regular user operation started in early 2019. After the installation and commissioning of all required components and a careful optimization of the electron beam, SwissFEL achieved its design parameters according to its Conceptual Design Report (CDR)[24] at the beginning of 2019, generating FEL pulses up to 500 μJ with a wavelength of 1 Å at a repetition rate of 100 Hz.

Results

Design. FEL radiation is generated by a high-charge-density electron beam travelling through an undulator beamline. The fundamental wavelength, λ, is given by[19]

$$\lambda = \frac{\lambda_u}{2\gamma^2}\left(1 + \frac{K^2}{2}\right) \quad (1)$$

where λ_u is the period length of the undulator, K is the undulator deflection parameter and γ is the Lorentz factor of the electron beam.

The challenge in the design of SwissFEL was to produce hard X-ray FEL radiation down to 1 Å with a substantially smaller footprint and cost than other facilities of comparable scientific potential. To achieve this, the most important design choice is to operate the facility at a relatively low electron beam energy (γ), which implies, according to equation (1), employing in-vacuum undulators with a short undulator period (λ_u): SwissFEL produces 1-Å FEL radiation with an electron beam energy of 5.8 GeV and an undulator period of 15 mm. The design philosophy of operating at low beam energies with short-period in-vacuum undulators to reach a certain wavelength was pioneered by Japanese colleagues at SPring 8, first with SCSS[25] for the extreme ultraviolet region and later with SACLA[21] for hard X-rays. Transversely coherent FEL radiation is produced if $\varepsilon_n/\gamma \lesssim \lambda/4\pi$, where ε_n is the normalized (transverse) electron beam emittance. Because SwissFEL produces radiation at 1 Å at a lower beam energy than existing FEL facilities, it requires an electron beam with smaller normalized emittance.

To further reduce the length and cost of the facility, the main linac was designed to achieve an optimum compromise between high accelerating gradient (implying smaller footprint and lower investment costs) and low power consumption (implying lower operational costs). This was realized by three main choices: first, adoption of C-band accelerating modules operating at 5.7 GHz to obtain a reliable accelerating gradient with a limited number of klystrons and modulators to reduce operating costs and to increase reliability; second, maximization of the effective shunt impedance of the RF system consisting of a barrel-open-cavity-type RF pulse compressor[26] and four 2-m-long accelerating structures per station[27]; third, use of solid-state modulators for driving the klystrons to increase the stability and reliability of the entire linac. The chosen optimum accelerating gradient is 28 MV m^{-1}, corresponding to a total of 26 RF stations to reach the final electron beam energy of 5.8 GeV. In total, SwissFEL employs 32 RF stations for beam acceleration (6 in the injector and 26 in the main linac). At 100-Hz operation and nominal beam parameters, the total power consumption of the facility amounts to just 1.7 MW.

Finally, the combination of a short-period undulator and a high-quality electron beam results in a short FEL gain length, provided that the undulator field sufficiently couples the electrons and photons. Consequently, the length of the undulator beamline required to achieve FEL saturation is relatively short in the SwissFEL case: the undulator beamline consists of only 13 modules with a length of 4 m each.

In short, SwissFEL is currently the hard X-ray FEL facility operating at the lowest electron beam energy (around 6 GeV) with the shortest undulator period (15 mm) and the shortest undulator beamline (52 m of effective undulator length). This represents an important further reduction in beam energy and undulator dimensions with respect to SACLA, which operates at 8.5-GeV beam energy with an undulator period of 18 mm and an effective undulator length of 90 m.

Table 1 shows the length, the final electron beam energy and the number of pulses per second of all hard X-ray FEL facilities (see https://www.xfel.eu/facility/comparison/index_eng.html). The total length of SwissFEL is 740 m, equivalent to SACLA and much shorter than other hard X-ray facilities. As a result of operating at the lowest electron beam energy, SwissFEL also features the lowest investment cost of all hard X-ray FELs[28]. The operational costs are another important consideration, being directly related to the power consumption of the facility. Thanks to the low electron beam energy, the efficient C-band technology and the chosen accelerating gradient, SwissFEL draws only 1.7 MW of power at 100-Hz operation, certainly less than any other hard X-ray facility. Increasing the accelerating gradient would allow for a further reduction of the facility footprint and hence construction costs, albeit at the expense of higher operational costs.

Figure 1 shows a sketch of SwissFEL. The electron source is a photocathode RF gun[29]. A frequency-quadrupled ytterbium calcium fluoride (Yb:CaF_2) laser[30] generates electrons via the photoelectric effect in a caesium telluride cathode deposited on a copper plug. An S-band (3 GHz) RF gun[31] accelerates the electrons to an energy of 7.1 MeV. The produced electron beam has a peak current of ~20 A, a typical charge of 200 pC, as well as low energy spread and emittance.

Table 1 | Facility length, electron beam energy and pulses per second of existing hard X-ray FELs

Parameter	LCLS	SACLA	PAL-XFEL	European XFEL	SwissFEL
Length (km)	3.0	0.75	1.1	3.4	0.74
Electron energy (GeV)	14.3	8.5	10	17.5	5.8
Pulses per second	120	60	60	27,000	100

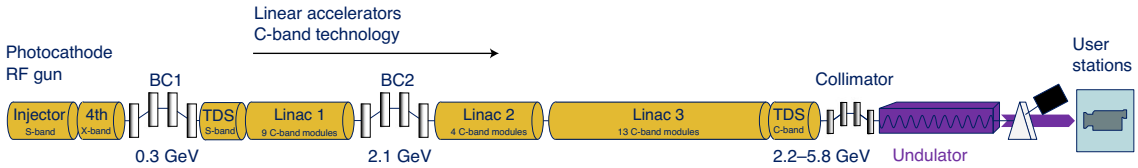

Fig. 1 | Schematic of SwissFEL. The schematic is not to scale. BC, bunch compressor; TDS, transverse-deflecting structure.

The 2.5-cell RF gun, inspired by the designs of the CTF3 drive beam[32] and the LCLS[33] guns, was designed to operate reliably at a gradient of 100 MV m^{-1} with a 100-Hz repetition rate for a balanced on-axis electric field and minimum field distortions. The main features adopted to achieve this are as follows: the middle cell is coupled to two rectangular waveguides, symmetrically arranged to cancel the dipole RF field components; the racetrack interior shape of the middle cell is optimized to minimize the quadrupole field components, the mode separation between the operating π mode and the π/2 next lower mode is higher than 15 GHz, and the RF coupling port dimensions were chosen to minimize thermal stress. In addition to the large mode separations, the effect of coupling the RF input waveguides on the middle cell is to inhibit excitation of the π/2 mode and, consequently, to further decrease the mode beating. Moreover, the solenoid magnet next to the gun is equipped with a quadrupole and a skew quadrupole magnet, enabling the compensation of possible quadrupole field distortions.

In the injector section, the beam is accelerated with S-band technology up to ~300 MeV. In our injector design[34], to achieve the best emittance, the distance between the gun and the first booster structure was chosen to be 20 cm longer than in the LCLS configuration (see ref. [35] and references therein). The beam is compressed in the first bunch compressor (BC1) by a factor close to 10 to reach peak currents of ~150 A. An X-band (12 GHz) RF structure[36], operating at the fourth harmonic of the S-band, linearizes the longitudinal phase space for optimum compression[37]. In the main linac, based on C-band technology, the beam is further accelerated to its final energy of up to ~6 GeV. The second bunch compressor (BC2) after linac 1 brings the electron beam to its final pulse length, with peak currents around 2–3 kA. Two transverse-deflecting structures (TDS) are used to diagnose the electron beam after each bunch compression stage (Methods). The undulator beamline consists of 13 undulator modules with variable gap, each of them with a total length of 4 m, a period of 15 mm and a minimum gap of 3 mm. After the electron beam has produced FEL radiation, it is deflected to the beam dump, while the FEL pulses propagate to the experimental stations. The wavelength range of the hard X-ray beamline of SwissFEL ranges from 1 to 7 Å (equivalent to a photon energy from ~2 to 12 keV). The shortest wavelength can be achieved with an electron beam energy of ~6 GeV and an undulator K parameter of ~1.2–1.3. The longer wavelengths are obtained by increasing the K parameter and/or reducing the beam energy.

The photon beam is distributed by X-ray optical mirrors to three hard X-ray experimental stations, of which two are currently in operation (Alvra and Bernina) and one is scheduled for operation in 2022 (Cristallina). Both operative hard X-ray photon beamlines are designed for flexible photon delivery[38], including mirrors delivering the full SASE bandwidth and monochromators for narrower bandwidth. The two stations feature amplified femtosecond laser systems[39] for ultrafast pump–probe experiments. The available pump laser infrastructure offers a broad range of output modes. These are based on two redundant amplified Ti:sapphire laser systems with up to 20 mJ of output energy and 30-fs pulse duration operating at 100 Hz. With subsequent nonlinear conversion stages, the output pulses can be tuned from ultraviolet to terahertz radiation. Alternatively, nonlinear pulse compression can provide pulse durations below 10 fs at 800 nm (ref. [39]). Moreover, both experimental stations are equipped with flexible Kirkpatrick–Baez mirrors to achieve micrometre-scale achromatic X-ray focusing and large-area 16-Mpixel Jungfrau detectors with dynamic gain switching technology[40].

Alvra focuses on ultrafast photochemistry and photobiology over the full photon energy range of the facility[41]. It takes advantage of a variety of X-ray techniques, primarily X-ray spectroscopy, X-ray scattering and serial femtosecond crystallography (SFX)[42], using a range of liquid and viscous sample delivery injectors. Bernina focuses on beyond-equilibrium ultrafast phenomena in condensed matter to advance the understanding of the subtle interplay among charge, orbital, spin and lattice degrees of freedom in modern materials[43]. To this end, a flexible diffractometer platform allows applying different resonant and non-resonant diffraction and scattering techniques in combination with heavy load sample environments such as low-temperature cryostats or magnets. The available pump laser extending to the terahertz range permits studies of low-energetic vibrational and/or magnetic excitations. Bernina also hosts the SwissMX instrument for fixed target SFX. More detailed information about the SwissFEL facility is available in refs. [24,44].

Table 2 | Design and measured parameters at SwissFEL

Parameter	Design	Measured
Electron beam energy (GeV)	5.8	6.2
Electron beam charge (pC)	200	200
Electron peak current (kA)	2.7	2.7
Electron beam slice emittance (nm)	430	200
Electron beam projected emittance (nm)	650	400
Electron beam slice energy spread (keV)	350	750
FEL radiation wavelength (Å)	1	1
FEL pulse energy at 1 Å (μJ)	150	600
FEL gain length at 1 Å (m)	-	2.3
Pulse repetition rate (Hz)	100	100

Electron and photon beam properties. Table 2 presents the original design[24] and measured electron and photon beam parameters for SwissFEL. Almost all design parameters foreseen in the CDR have been achieved or surpassed. The exception is the slice energy spread of the electron beam, which is about twice the design value. This can be attributed to an underestimation of the initial beam energy spread at the gun exit, to some deterioration effect such as microbunching[45] or to detector resolution. Despite a larger beam energy spread, the overall beam quality is improved substantially due to much smaller emittance, allowing a higher pulse energy than the values foreseen in the SwissFEL CDR. Although the accelerator achieves peak currents at the design value (2.7 kA) or above, we typically obtain better FEL performance at somewhat reduced currents (about 2 kA).

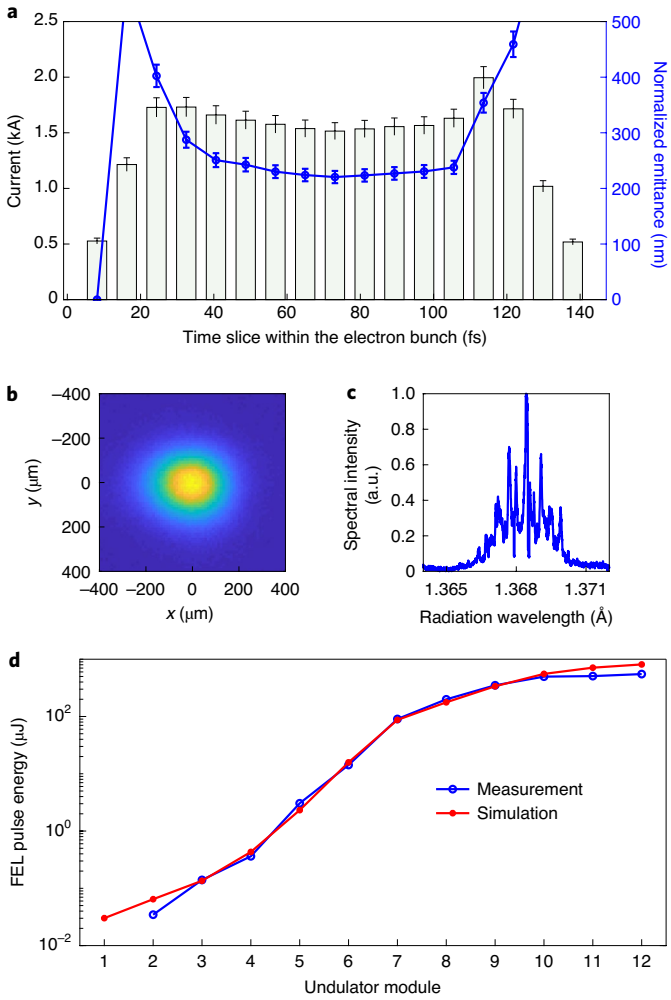

Fig. 2 | Electron and photon beam properties at SwissFEL. a, Longitudinal profile and slice emittance measurement of the electron beam. The error bars represent one standard deviation of uncertainty. **b**, Typical transverse profile of the FEL radiation 53 m downstream of the last undulator module for a radiation wavelength of 1.4 Å. **c**, Typical spectrum of the FEL pulses for a central wavelength of ~1.4 Å. **d**, Measured (blue) and simulated (red) FEL pulse energy along the undulator beamline for a radiation wavelength of 1.0 Å.

Figure 2a shows a typical measurement at the undulator entrance of the current and the transverse emittance along the longitudinal position within the electron bunch. The longitudinal profile is rather flat with a current between 1.5 and 2 kA and an electron bunch duration of ~30 fs (root mean square (r.m.s.)). The emittance for a longitudinal fraction of the bunch, that is, the slice emittance, is ~200 nm for the beam core.

These emittance values are possible thanks to several factors. First, the RF gun and the injector, as described earlier, were carefully designed to achieve optimum emittances. Second, we employ caesium telluride cathodes, with small intrinsic emittance and high quantum efficiency[46], allowing use of the excess laser pulse energy to improve the quality of the laser transverse profile by spatial filtering. Third, we implement a careful set-up to minimize emittance at the injector and to preserve it through compression (Methods). Finally, we have a robust, precise and high-resolution measurement procedure capable of characterizing our low-emittance beams. More information about emittance optimization and measurements at SwissFEL is available in refs. [34,47,48]. The generation of electron beams with low emittance at the injector (and its good preservation after compression) is one of the outstanding features of SwissFEL.

SwissFEL produces FEL radiation with pulse energies of more than 500 μJ for the full design wavelength range. Record pulse energies reached so far are around 800 μJ for a radiation wavelength of 1.7 Å and around 900 μJ for a wavelength of 3.4 Å. The electron bunch duration is typically between 20 and 35 fs (r.m.s.). However, shorter bunches at the femtosecond level can be achieved by strongly compressing low-charge electron beams. Because the electron beam is not lasing over its full length, the photon beam durations must be shorter. The relative FEL bandwidth can routinely be controlled between 0.05 and 0.2% (r.m.s.). Figure 2b,c shows a typical example of an FEL transverse profile and spectrum for a radiation wavelength of 1.4 Å. For this particular case, the relative bandwidth is 0.1% (r.m.s.).

The measured FEL performance matches simulations, as shown in the gain curve in Fig. 2d for a radiation wavelength of 1.0 Å. For the example shown in the figure, the first undulator was not aligned and therefore was not contributing to the FEL process. We determined a final pulse energy of 550 μJ and a gain length of 2.3 m. The simulated gain curve, obtained from measured electron beam parameters with the code Genesis 1.3[49], reproduces the experimental measurement both qualitatively and quantitatively. The pulse energy was matched assuming that 50% of the bunch is contributing to the FEL process. In the measurement shown in Fig. 2a, ~65% of the bunch has suitable emittance and current to efficiently drive the FEL process. The 15% difference can be explained by a slice trajectory misalignment or by the fact that undulator wakefields were not well compensated by tapering at the head and tail of the bunch. The final pulse energy is higher in simulations than in measurements. This discrepancy can be attributed to a non-optimal post-saturation tapering configuration during the experiment.

Thanks to the stability of the accelerator components and the efficient use of feedback, the electron and photon pulse trains of SwissFEL are comparatively stable. The following stability figures refer to r.m.s. values. The short-term stability or jitter in pulse energy is typically below 10%. The photon pulse pointing jitter is typically ≤10% of the transverse beam size at the far distance. The relative electron energy jitter is ~10^{-4}, corresponding to a relative central wavelength jitter of ~2×10^{-4}. The arrival-time jitter of the electron beam, as measured by the TDS at the end of the linac, is less than 10 fs. Beam-based feedback (Methods) ensure the performance stability of SwissFEL also on longer timescales.

Good control of the time delay between pump laser and FEL pulses is of paramount importance for pump–probe set-ups at the experimental stations. At SwissFEL it is possible to measure vibrational frequencies up to a few terahertz. One example is the measurement of coherent optical phonons in crystalline bismuth[50], as shown in Fig. 3, where ultrafast timing diagnostics have been employed to measure the relative time between pump and FEL pulses and bin the data accordingly.

First demonstration of experimental capabilities. The first pilot experiments at SwissFEL were successfully performed at the end of 2017. At Bernina, a pump–probe powder diffraction measurement revealed the picosecond dynamics during a phase transition in nanocrystallites of Ti_3O_5 using the third harmonic of the FEL at 6.6 keV (ref. [43]). At Alvra, the ultrafast phosphorus K-edge X-ray emission of a Cu- and P-based organic light-emitting diode material was measured at 2.2 keV to probe the charge-transfer character of the excited state's thermally activated delayed fluorescence[51].

In the course of 2018, further pilot experiments utilizing the specialization of the experimental stations enabled new scientific insights. The achievements in 2018 include the measurement of terahertz excited structural dynamics of a ferroelectric material[43], the first resonant tender X-ray diffraction on magnetic and elec-

tronic dynamics in a ruthenate, a protein SFX phasing experiment performed at 4.5 keV to enhance the anomalous scattering signal from a GPCR membrane protein, and the first X-ray transient grating pump–optical-probe experiment extending the four-wave mixing technique to hard X-rays[52].

SwissFEL began regular user operation in January 2019. Among the first official experiments, we highlight the ultrafast SFX studies that enabled the assembly of a molecular movie of structural dynamics in a sodium pump, thus providing direct insight into the mechanism underlying cation transport across biological membranes[53].

Special operation modes. Beyond its standard operation mode, SwissFEL provides special control of some radiation parameters, namely pulse duration and spectral properties. We operate at an electron beam charge of 10 pC to obtain shorter pulses than in the standard configuration. In contrast to regular operation, where the beam is longitudinally compressed with two bunch compressors, the generation of ultra-short pulses additionally makes use of the energy collimator as a third bunch compressor. Because this chicane is placed just before the undulator beamline, we can fully compress the beam while avoiding detrimental space-charge forces. This set-up allows us to generate ultra-short pulses with enhanced stability. Figure 4a shows examples of single-shot spectral measurements with one or two spikes or modes[54,55], indicating pulse durations well below 1 fs. An analysis of the pulse duration based on the spike width of the spectra[56] shows that our pulses can be as short as 100 as (r.m.s. values). These values are obtained under the assumption of no energy chirp, which was minimized during the experiment by adjusting the linac phase (the pulse duration obtained with the spectral method can be underestimated up to a factor of $\sqrt{2}$ in the presence of an energy chirp[57]). The pulse energy of these short pulses is typically on the order of a few microjoules. Short FEL radiation has potential benefits for many applications, for instance in SFX. We note that the generation of sub-femtosecond FEL pulses has previously been achieved at LCLS for both soft and hard X-rays[57–59].

Another special configuration mode allows us to provide users with large-bandwidth radiation, which is desirable, for example, to substantially improve the efficiency of certain techniques such as X-ray crystallography and spectroscopy[60]. We obtain broadband pulses by maximizing the energy chirp of the electron beam at the undulator entrance. Thanks to the unique combination of the strong linac wakefields and the low-energy electron beam, SwissFEL can generate FEL pulses with unprecedented bandwidth up to 2% for a radiation wavelength of ~1 Å, as shown in Fig. 4b. The pulse energy in the large-bandwidth operation mode is equivalent to the one obtained in the standard configuration. More details on the generation of large-bandwidth radiation at SwissFEL are provided in ref. [61].

SwissFEL can also produce two-colour FEL pulses by applying several methods. In particular, we recently demonstrated a new and simple approach to generate two-colour radiation that requires only one sextupole magnet[62]. The generation of two-colour radiation may be useful for X-ray pump–X-ray probe experiments—see, for example, ref. [63].

Summary. We have presented the first lasing results from SwissFEL, the most compact and cost-effective hard X-ray FEL facility so far. SwissFEL is driven by an electron beam with the lowest energy and emittance compared to existing hard X-ray FEL facilities. Hard X-ray radiation with pulse energies of more than 500 μJ, pulse durations of ~30 fs (r.m.s.) and spectral bandwidth below the per-mil level have been demonstrated. Special operation modes provide pulses shorter than 1 fs and broadband radiation with bandwidth around 2%. Even with the lowest electron beam energy and therefore the lowest electron beam power among all hard X-ray FELs, pulse energies comparable to the higher-energy facilities can be reached routinely, thanks to the high brightness of the electron beam.

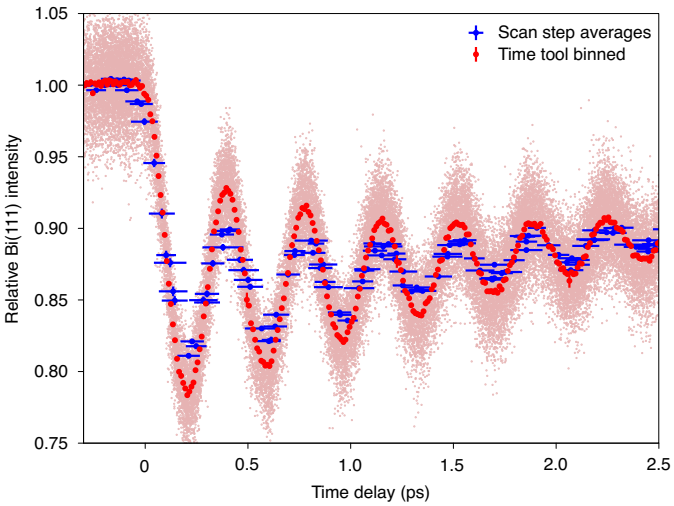

Fig. 3 | Transient response in Bi(111) peak intensity displaying a coherent optical phonon, displacively excited by an 800-nm pulse. The data were recorded by scanning the arrival time of the pump pulses using a translation stage, while simultaneously measuring, shot-by-shot, the relative laser to X-ray pulse arrival time jitter using a 'spatial encoding' timing tool[70]. Plotting each delay step averaged both in X-ray intensity and corrected time delay demonstrates the effect of time delay jitter and drift (blue points; the horizontal error bars correspond to one standard deviation of the time delay jitter). After correcting single pulses for time delay (light dots), the data have been averaged into 10-fs bins (red). The vertical error bars correspond to binned statistics of one standard deviation divided by the square root of the number of pulses in each bin.

Discussion

In principle, the electron beam generated at SwissFEL, with its unprecedented low emittance substantially below the original design goals, could drive an ångström-wavelength FEL at even lower beam energies of ~4.5 GeV (ref. [48]) (assuming feasible undulators with periods shorter than 10 mm; ref. [64]). Alternatively, staying at the present electron beam energy, the wavelength range of SwissFEL could be extended towards shorter wavelengths. These results pave the way to yet more compact and affordable FELs, such as the upcoming CompactLight project (http://www.compactlight.eu), which may boost the number of such facilities, thereby expanding the accessibility of the user community to hard X-ray FEL radiation. Accordingly, further growth in X-ray FEL science as well as potential industrial or medical applications may be envisioned.

In the near future. we plan to study new approaches to produce short and two-colour pulses with enhanced tunability with respect to the methods described in the section 'Special operation modes'. To this effect, we will explore the generation of short pulses by inducing a transverse chirp to the electron beam[65]. This method will give us better control of the pulse duration, which can be changed simply by tuning the amplitude of the beam tilt. Moreover, we will produce two-colour FEL pulses with two undulator sections tuned to different radiation wavelengths and a chicane between them[66]. This will allow for larger tunability in both time and wavelength separation between the two pulses.

At present, the second accelerator beamline of SwissFEL, dedicated to soft X-ray radiation in the wavelength range between 0.65 and 5.0 nm, is under installation and commissioning. Thanks to the two-bunch operation and a fast bunch separation system, the soft X-ray beamline will be served up to the full SwissFEL repetition rate without disturbing the hard X-ray branch[67]. This beamline will consist of Apple-X undulators capable of providing full polarization control and transverse gradient control[68]. This flexible undulator

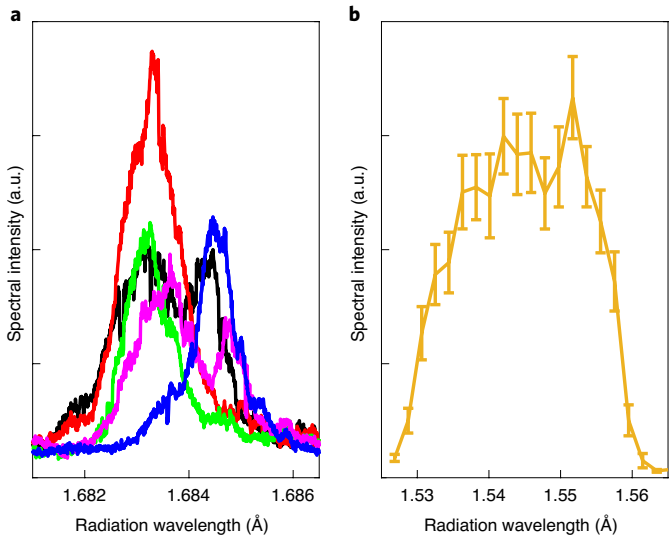

Fig. 4 | SwissFEL special operation modes. a, Ultra-short pulses: five consecutive single-shot spectral measurements with one or two spikes, indicating FEL radiation with a duration below 1 fs. **b**, Large-bandwidth configuration: average spectrum measurement showing a total bandwidth larger than 2%. The error bars correspond to one standard deviation of uncertainty.

configuration and the installation of inter-undulator chicanes will allow for many unique operational modes, giving control over FEL properties such as peak power, pulse duration and longitudinal coherence[69]. We intend to offer soft X-ray FEL radiation to scientific users from 2021, with two facility-supported experimental stations: one dedicated to atomic, molecular and optical physics and a second dedicated to condensed matter physics and materials investigation.

Online content

Any methods, additional references, Nature Research reporting summaries, source data, extended data, supplementary information, acknowledgements, peer review information; details of author contributions and competing interests; and statements of data and code availability are available at https://doi.org/10.1038/s41566-020-00712-8.

Received: 24 January 2020; Accepted: 30 September 2020;
Published online: 9 November 2020

References

1. McNeil, B. W. J. & Thompson, N. R. X-ray free-electron lasers. *Nat. Photon.* **4**, 814–821 (2010).
2. Pellegrini, C., Marinelli, A. & Reiche, S. The physics of X-ray free-electron lasers. *Rev. Mod. Phys.* **88**, 015006 (2016).
3. Bostedt, C. et al. Linac Coherent Light Source: the first five years. *Rev. Mod. Phys.* **88**, 015007 (2016).
4. Kern, J. et al. Simultaneous femtosecond X-ray spectroscopy and diffraction of photosystem II at room temperature. *Science* **340**, 491–495 (2013).
5. Nango, E. et al. A three-dimensional movie of structural changes in bacteriorhodopsin. *Science* **354**, 1552–1557 (2016).
6. Nogly, P. et al. Retinal isomerization in bacteriorhodopsin captured by a femtosecond X-ray laser. *Science* **361**, eaat0094 (2018).
7. Dell'Angela, M. et al. Real-time observation of surface bond breaking with an X-ray laser. *Science* **339**, 1302–1305 (2013).
8. Öström, H. et al. Probing the transition state region in catalytic CO oxidation on Ru. *Science* **347**, 978–982 (2015).
9. Graves, C. E. et al. Nanoscale spin reversal by non-local angular momentum transfer following ultrafast laser excitation in ferrimagnetic GdFeCo. *Nat. Mater.* **12**, 293–298 (2013).
10. Beaud, P. et al. A time-dependent order parameter for ultrafast photoinduced phase transitions. *Nat. Mater.* **13**, 923–927 (2014).
11. Dornes, C. et al. The ultrafast Einstein–de Haas effect. *Nature* **565**, 209–212 (2019).
12. Liu, W. et al. Serial femtosecond crystallography of G protein-coupled receptors. *Science* **342**, 1521–1524 (2013).
13. Redecke, L. et al. Natively inhibited *Trypanosoma brucei* cathepsin B structure determined by using an X-ray laser. *Science* **339**, 227–230 (2012).
14. Kang, Y. et al. Crystal structure of rhodopsin bound to arrestin by femtosecond X-ray laser. *Nature* **523**, 561–567 (2015).
15. Glover, T. E. et al. X-ray and optical wave mixing. *Nature* **488**, 603–608 (2012).
16. Tamasaku, K. et al. X-ray two-photon absorption competing against single and sequential multiphoton processes. *Nat. Photon.* **8**, 313–316 (2014).
17. Szlachetko, J. et al. Establishing nonlinearity thresholds with ultraintense X-ray pulses. *Sci. Rep.* **6**, 33292 (2016).
18. Kondratenko, A. M. & Saldin, E. L. Generation of coherent radiation by a relativistic electron beam in an ondulator. *Part. Accel.* **10**, 207–216 (1980).
19. Bonifacio, R., Pellegrini, C. & Narducci, L. M. Collective instabilities and high-gain regime in a free electron laser. *Opt. Commun.* **50**, 373 –378 (1984).
20. Emma, P. et al. First lasing and operation of an ångström-wavelength free-electron laser. *Nat. Photon.* **4**, 641–647 (2010).
21. Ishikawa, T. et al. A compact X-ray free-electron laser emitting in the sub-ångström region. *Nat. Photon.* **6**, 540–544 (2012).
22. Kang, H.-S. et al. Hard X-ray free-electron laser with femtosecond-scale timing jitter. *Nat. Photon.* **11**, 708–713 (2017).
23. Decking, W. et al. A MHz-repetition-rate hard X-ray free-electron laser driven by a superconducting linear accelerator. *Nat. Photon.* **14**, 391–397 (2020).
24. Ganter, R. et al. *SwissFEL Conceptual Design Report* PSI Report 10-04 (Paul Scherrer Institut, 2012).
25. Shintake, T. et al. A compact free-electron laser for generating coherent radiation in the extreme ultraviolet region. *Nat. Photon.* **2**, 555–559 (2008).
26. Zennaro, R., Bopp, M., Citterio, A., Reiser, R. & Stapf, T. C-band RF pulse compressor for SwissFEL. In *Proceedings of the 4th International Particle Accelerator Conference* 2827–2829 (JACoW Publishing, 2013).
27. Raguin, J.-Y. & Bopp, M. The Swiss FEL C-band accelerating structure: RF design and thermal analysis. In *Proceedings of LINAC 2012*, 501–503 (JACoW Publishing, 2013).
28. Cartlidge, E. European XFEL to shine as brightest, fastest X-ray source. *Science* **354**, 22–23 (2016).
29. Fraser, J. S., Sheffield, R. L., Gray, E. R. & Rodenz, G. W. High-brightness photoemitier injector for electron accelerators. *IEEE Trans. Nucl. Sci.* **32**, 1791–1793 (1985).
30. Trisorio, A., Divall, M., Vicario, C., Hauri, C. P. & Courjaud, A. New concept for the SwissFEL gun laser. In *Proceedings of FEL 2013*, Vol. 35, 442–446 (JACoW Publishing, 2013).
31. Raguin, J.-Y., Bopp, M., Citterio, A. & Scherer, A. The Swiss FEL RF gun: RF design and thermal analysis. In *Proceedings of 26th International Linear Accelerator Conference 2012*, 442–444 (JACoW Publishing, 2013).
32. Roux, R. Conception of photoinjectors for the CTF3 experiment. *Int. J. Mod. Phys. A* **22**, 3925–3941 (2007).
33. Xiao, L. et al. Dual feed RF gun design for the LCLS. In *Proceedings of the 2005 Particle Accelerator Conference* 3432–3434 (IEEE, 2005).
34. Bettoni, S., Pedrozzi, M. & Reiche, S. Low emittance injector design for free electron lasers. *Phys. Rev. ST Accel. Beams* **18**, 123403 (2015).
35. Ferrario, M. et al. Direct measurement of the double emittance minimum in the beam dynamics of the sparc high-brightness photoinjector. *Phys. Rev. Lett.* **99**, 234801 (2007).
36. Dehler, M. et al. X-band rf structure with integrated alignment monitors. *Phys. Rev. ST Accel. Beams* **12**, 062001 (2009).
37. Dowell, D. H., Hayward, T. D. & Vetter, A. M. Magnetic pulse compression using a third harmonic RF linearizer. In *Proceedings of the 1995 Particle Accelerator Conference* 992–994 (IEEE, 1996).
38. Follath, R. et al. Optical design of the ARAMIS-beamlines at SwissFEL. In *Proceedings of the 12th International Conference on Synchrotron Radiation Instrumentation*, Vol. 1741, 020009 (AIP, 2016).
39. Erny, C. & Hauri, C. P. The SwissFEL experimental laser facility. *J. Synchrotron Radiat.* **23**, 1143–1150 (2016).
40. Redford, S. et al. Operation and performance of the JUNGFRAU photon detector during first FEL and synchrotron experiments. *J. Instrum.* **13**, C11006 (2018).
41. Milne, C. et al. Opportunities for chemistry at the SwissFEL X-ray free electron laser. *CHIMIA Int. J. Chem.* **71**, 299–307 (2017).
42. Chapman, H. N. et al. Femtosecond X-ray protein nanocrystallography. *Nature* **470**, 73–77 (2011).
43. Ingold, G. et al. Experimental station Bernina at SwissFEL: condensed matter physics on femtosecond time scales investigated by X-ray diffraction and spectroscopic methods. *J. Synchrotron Radiat.* **26**, 874–886 (2019).

44. Milne, C. J. et al. SwissFEL: the Swiss X-ray Free Electron Laser. *Appl. Sci.* **7**, 720 (2017).
45. Heifets, S., Stupakov, G. & Krinsky, S. Coherent synchrotron radiation instability in a bunch compressor. *Phys. Rev. ST Accel. Beams* **5**, 064401 (2002).
46. Prat, E., Bettoni, S., Braun, H.-H., Ganter, R. & Schietinger, T. Measurements of copper and cesium telluride cathodes in a radio-frequency photoinjector. *Phys. Rev. ST Accel. Beams* **18**, 043401 (2015).
47. Prat, E. et al. Emittance measurements and minimization at the SwissFEL injector test facility. *Phys. Rev. ST Accel. Beams* **17**, 104401 (2014).
48. Prat, E. et al. Generation and characterization of intense ultralow-emittance electron beams for compact X-ray free-electron lasers. *Phys. Rev. Lett.* **123**, 234801 (2019).
49. Reiche, S. GENESIS 1.3: a fully 3D time-dependent FEL simulation code. *Nucl. Instrum. Methods Phys. Res. A* **429**, 243–248 (1999).
50. Sokolowski-Tinten, K. et al. Femtosecond X-ray measurement of coherent lattice vibrations near the Lindemann stability limit. *Nature* **422**, 287–289 (2003).
51. Smolentsev, G. et al. Taking a snapshot of the triplet excited state of an OLED organometallic luminophore using X-rays. *Nat. Commun.* **11**, 2131 (2020).
52. Svetina, C. et al. Towards X-ray transient grating spectroscopy. *Opt. Lett.* **44**, 574–577 (2019).
53. Skopintsev, P. et al. Femtosecond-to-millisecond structural changes in a light-driven sodium pump. *Nature* **583**, 314–318 (2020).
54. Saldin, E. L., Schneidmiller, E. A. & Yurkov, M. V. Statistical properties of radiation from VUV and X-ray free electron laser. *Opt. Commun.* **148**, 383–403 (1998).
55. Ayvazyan, V. et al. Study of the statistical properties of the radiation from a VUV SASE FEL operating in the femtosecond regime. *Nucl. Instrum. Methods Phys. Res. A* **507**, 368–372 (2003).
56. Inubushi, Y. et al. Determination of the pulse duration of an X-ray free electron laser using highly resolved single-shot spectra. *Phys. Rev. Lett.* **109**, 144801 (2012).
57. Huang, S. et al. Generating single-spike hard X-ray pulses with nonlinear bunch compression in free-electron lasers. *Phys. Rev. Lett.* **119**, 154801 (2017).
58. Marinelli, A. et al. Experimental demonstration of a single-spike hard-X-ray free-electron laser starting from noise. *Appl. Phys. Lett.* **111**, 151101 (2017).
59. Duris, J. et al. Tunable isolated attosecond X-ray pulses with gigawatt peak power from a free-electron laser. *Nat. Photon.* **14**, 30–36 (2019).
60. Patterson, B. D. et al. Coherent science at the SwissFEL X-ray laser. *New J. Phys.* **12**, 035012 (2010).
61. Prat, E., Dijkstal, P., Ferrari, E. & Reiche, S. Demonstration of large bandwidth hard X-ray free-electron laser pulses at SwissFEL. *Phys. Rev. Lett.* **124**, 074801 (2020).
62. Dijkstal, P., Malyzhenkov, A., Reiche, S. & Prat, E. Demonstration of two-color X-ray free-electron laser pulses with a sextupole magnet. *Phys. Rev. Accel. Beams* **23**, 030703 (2020).
63. Inoue, I. et al. Observation of femtosecond X-ray interactions with matter using an X-ray–X-ray pump–probe scheme. *Proc. Natl Acad. Sci. USA* **113**, 1492–1497 (2016).
64. Calvi, M. et al. A GdBCO bulk staggered array undulator. *Supercond. Sci. Technol.* **33**, 014004 (2020).
65. Prat, E., Bettoni, S. & Reiche, S. Enhanced X-ray free-electron-laser performance from tilted electron beams. *Nucl. Instrum. Methods Phys. Res. A* **865**, 1–8 (2017).
66. Lutman, A. A. et al. Fresh-slice multicolour X-ray free-electron lasers. *Nat. Photon.* **10**, 745–750 (2016).
67. Paraliev, M. et al. Commissioning and stability studies of the SwissFEL bunch-separation system. In *Proceedings of the 2009 Free Electron Laser Conference* 404–407 (JACoW Publishing, 2019).
68. Schmidt, T. & Calvi, M. APPLE X undulator for the SwissFEL soft X-ray beamline athos. *Synchrotron Radiat. News* **31**, 35–40 (2018).
69. Abela, R. et al. The SwissFEL soft X-ray free-electron laser beamline: Athos. *J. Synchrotron Radiat.* **26**, 1073–1084 (2019).
70. Harmand, M. et al. Achieving few-femtosecond time-sorting at hard X-ray free-electron lasers. *Nat. Photon.* **7**, 215–218 (2013).

Methods

Machine set-up. FEL performance is determined by the electron density in six-dimensional phase space. The machine set-up mainly consists of optimization of the transverse emittance, compression of the electron beam in two bunch-compressor stages, the optics set-up, beam-based alignment (BBA) of the electron beam to ensure a suitable transverse overlap between the electron and photon beams, and the set-up of the undulator modules.

We first optimize the quality of the RF photo-injector beam, essentially following the procedure described in ref. [47]. The transverse profile of the gun laser beam is optimized for maximum homogeneity and symmetry. Its longitudinal profile has a Gaussian shape with an r.m.s. width of ~3 ps, resulting in approximately the same electron pulse duration and a peak current of ~20 A for the standard beam charge of 200 pC. The RF gun parameters are tuned by means of a magnetic spectrometer, where the gradient is set to its maximum operational value of 100 MV m^{-1} to provide an electron beam energy of 7.1 MeV, and the phase is set to minimize the electron beam energy spread. The laser beam diameter at the cathode and the gun solenoid field are set to design values[34] and then slightly tuned for minimum emittance. If necessary, the transverse coupling is also measured and minimized. Finally, the electron beam trajectory is aligned with respect to various components (for example, magnets and RF structures) to minimize dispersion and wakefield effects.

In a second step, we accelerate the beam in the injector and set up the first bunch-compression stage, which compresses the beam by a factor of about 7–8. We minimize the emittance growth associated with compression and transport by adopting three measures: we set adequate optics to ensure a small horizontal beam size at the last dipole of the chicane to minimize the degradation by coherent synchrotron radiation effects, we correct any possible transverse beam tilts by use of magnets in the bunch compressors according to ref. [71], and we align the beam within the RF structures and magnets. Afterwards, we further accelerate the beam and compress it to its final pulse duration in the second bunch compressor. There, we adopt the same measures as for the first bunch compressor to minimize the final electron beam emittance.

Once the electron beam is suitable for the FEL process, an undulator BBA is implemented to ensure a good transverse overlap between the electron and photon beams along the undulator line. For this we apply the methods outlined in refs. [72,73]. This is followed by setting up the undulator modules. These are aligned with respect to the golden trajectory found in the BBA, and the undulator K parameters are calibrated absolutely with the help of a monochromator and a multi-channel plate detector or a photodiode according to ref. [74]. Finally, a random-walk optimization of different relevant parameters is implemented to maximize the resulting pulse energy or to optimize the ratio between the pulse energy and the spectral bandwidth.

Electron diagnostics and feedback. Electron beam instrumentation in SwissFEL is used to prepare the electron beam for lasing and to maintain stable performance with beam-based feedback. The transverse emittances are reconstructed with the quadrupole scan technique, as described in refs. [47,75]. The transverse beam sizes required for the emittance reconstruction are mostly measured with screen monitors based on scintillating cerium-doped yttrium aluminium garnet (Ce:YAG) crystals[76]. Alternatively, we employ wire scanners for slow but high-resolution beam-size measurements[77]. The beam-size determination at dispersive locations (in bunch compressors and spectrometers) allows us to estimate the beam energy spread. SwissFEL is equipped with a synchrotron radiation monitor in each bunch compressor to non-invasively measure the energy distribution of the electron beam[78]. Two transverse-deflecting RF structures (TDSs)[79] are used in conjunction with profile monitors to measure the longitudinal profile, the slice emittance and the slice energy spread of the electron beam. An S-band TDS is placed downstream of the first bunch compressor to obtain the longitudinal beam properties with a resolution of ~10 fs. Downstream of the main linac there is a C-band TDS able to measure the longitudinal phase space with a time resolution of ~1 fs. The BBA is performed with cavity beam-position monitors (BPMs), which are able to measure the beam trajectory with sub-micrometre resolution[80]. Beam-loss monitors ensure radiation protection during accelerator operations and provide the signal to reconstruct the beam transverse profile in a wire-scanner measurement.

Beam-based feedback keeps the charge, energy, trajectory, compression and arrival time of the electron beam constant. The charge of the electron beam is measured with integrating current transformers (ICTs). BPMs are able to measure the relative bunch charge and are calibrated to match the ICTs. Energy and trajectory feedback is based on BPM measurements at dispersive and non-dispersive locations, respectively. The compression feedback relies on dedicated monitors, installed after each bunch-compression stage. These are sensitive to relative changes in bunch compression[81] and are based on the detection of coherent edge radiation and coherent diffraction radiation. Finally, bunch arrival-time monitors[82] are employed to measure and feed back the arrival time of the electron beam.

Photon diagnostics. We only briefly discuss the photon diagnostics involved in the characterization of the first SwissFEL lasing and refer to ref. [83] for more details on the full suite of SwissFEL photon diagnostics. The FEL pulse energy is measured with a photon beam intensity gas monitor. This gas-filled device non-destructively measures the average absolute pulse energy over several seconds and a relative pulse energy on a shot-to-shot basis by accelerating photoionized Xe, Kr or Ar atoms against a copper plate and measuring the resulting current. The absolute accuracy of this device is better than 10%.

The FEL spectrum is measured on a shot-to-shot non-destructive basis with a device that uses a diamond grating to split off a portion of the FEL beam onto a bent Si crystal where it is Bragg-reflected. The spectra are then projected through a He-filled tube onto a Ce:YAG screen mounted on a vertical rotatable stage and read out by a CMOS camera. The typical energy resolution of the spectrometer is between 2×10^{-5} and 5×10^{-5} with a field of view corresponding to ~0.5% of the photon energy. The spectrometer is designed to function at photon energies between 4 and 13 keV. For bandwidth larger than the spectrometer's field of view, we measure average spectra by scanning a monochromator[38] and recording the output intensity with a photodiode.

Photon profile monitors supply an image of the beam from a scintillating Ce:YAG crystal. These screens yield a resolution of ~11 μm and are used mainly to measure the radiation transverse profiles and trajectories in a destructive way. Owing to their large dynamic range, they are also employed to measure the relative photon pulse energy for FEL gain curve measurements. Further components include a photodiode and a spontaneous-radiation detector used for the undulator set-up, consisting of a multi-channel plate with a screen, a mirror and a camera.

Data availability

The data that support the figures in this paper and other findings of this study are available from the corresponding author upon reasonable request.

Code availability

The FEL code Genesis 1.3 is available at http://genesis.web.psi.ch.

References

71. Guetg, M. W., Beutner, B., Prat, E. & Reiche, S. Optimization of free electron laser performance by dispersion-based beam-tilt correction. *Phys. Rev. ST Accel. Beams* **18**, 030701 (2015).
72. Aiba, M. & Böge, M. Beam-based alignment of an X-FEL undulator section utilizing the corrector pattern. In *Proceedings of the 2012 Free Electron Laser Conference* 293–296 (JACoW Publishing, 2013).
73. Emma, P., Carr, R. & Nuhn, H.-D. Beam-based alignment for the LCLS FEL undulator. *Nucl. Instrum. Methods Phys. Res. A* **429**, 407–413 (1999).
74. Calvi, M. et al. General strategy for the commissioning of the ARAMIS undulators with a 3-GeV electron beam. In *Proceedings of the 2014 Free Electron Laser Conference* 107–110 (JACoW Publishing, 2015).
75. Prat, E. Symmetric single-quadrupole-magnet scan method to measure the 2D transverse beam parameters. *Nucl. Instrum. Methods Phys. Res. A* **743**, 103–108 (2014).
76. Ischebeck, R., Prat, E., Thominet, V. & Ozkan Loch, C. Transverse profile imager for ultrabright electron beams. *Phys. Rev. ST Accel. Beams* **18**, 082802 (2015).
77. Orlandi, G. L. et al. Design and experimental tests of free electron laser wire scanners. *Phys. Rev. Accel. Beams* **19**, 092802 (2016).
78. Orlandi, G. et al. Bunch length and energy measurements in the bunch compressor of a free-electron laser. *Phys. Rev. Accel. Beams* **22**, 072803 (2019).
79. Craievich, P., Ischebeck, R., Löhl, F., Orlandi, G. L. & Prat, E. Transverse deflecting structures for bunch length and slice emittance measurements on SwissFEL. In *Proceedings of the 2013 Free Electron Laser Conference* 236–241 (JACoW Publishing, 2013).
80. Keil, B. et al. First beam commissioning experience with the SwissFEL Cavity BPM system. In *Proceedings of the 2017 International Beam Instrumentation Conference* 251–254 (JACoW Publishing, 2017).
81. Frei, F. et al. Development of electron bunch compression monitors for SwissFEL. In *Proceedings of the 2013 International Beam Instrumentation Conference* 769–771 (JACoW Publishing, 2013).
82. Arsov, V. et al. First results from the bunch arrival-time monitors at SwissFEL. In *Proceedings of the 2018 International Beam Instrumentation Conference* 420–424 (JACoW Publishing, 2019).
83. Juranić, P. et al. SwissFEL Aramis beamline photon diagnostics. *J. Synchrotron Radiat.* **25**, 1238–1248 (2018).

Acknowledgements

We thank all the technical groups involved in the construction, installation and operation of SwissFEL. We also thank K. Sokolowski Tinten and M. Horn-von Hoegen for providing the thin-film Bi samples used in the timing characterization. This work has been supported by SNF grant no. 200021 175498 and no. 51NF40-183615 (NCCR:MUST). Moreover, this project has received funding from the European Research Council (ERC) under the European Union's Horizon 2020 research and innovation programme (grant agreement no. 695197 DYNAMOX).

Author contributions

E.P. wrote the initial version of the manuscript with the help of P.J., R.I., H.T.L., F.L., C.J.M., S. Reiche, T. Schietinger and H.-H.B. All authors contributed to the final version of the document. All authors participated in the design, construction or commissioning of SwissFEL. F.L. was the machine coordinator of SwissFEL. H.-H.B., R.A. and L.P. were the project leaders of SwissFEL.

Competing interests

The authors declare no competing interests.

Additional information

Correspondence and requests for materials should be addressed to E.P.

Reprints and permissions information is available at www.nature.com/reprints.